



**HAL**  
open science

## **$\kappa$ -Carrageenan Associated with Fructose/Glycerol/Water LTTM: Toward Natural Thermosensitive Physical Gels**

Benoit Caprin, Guadalupe Viñado-Buil, Guillaume Sudre, Xavier Morelle, Fernande da Cruz-Boisson, Aurélia Charlot, Etienne Fleury

► **To cite this version:**

Benoit Caprin, Guadalupe Viñado-Buil, Guillaume Sudre, Xavier Morelle, Fernande da Cruz-Boisson, et al..  $\kappa$ -Carrageenan Associated with Fructose/Glycerol/Water LTTM: Toward Natural Thermosensitive Physical Gels. ACS Sustainable Chemistry & Engineering, 2022, 10 (45), pp.14817-14825. 10.1021/acssuschemeng.2c04437 . hal-04144191

**HAL Id: hal-04144191**

**<https://hal.science/hal-04144191>**

Submitted on 24 Nov 2023

**HAL** is a multi-disciplinary open access archive for the deposit and dissemination of scientific research documents, whether they are published or not. The documents may come from teaching and research institutions in France or abroad, or from public or private research centers.

L'archive ouverte pluridisciplinaire **HAL**, est destinée au dépôt et à la diffusion de documents scientifiques de niveau recherche, publiés ou non, émanant des établissements d'enseignement et de recherche français ou étrangers, des laboratoires publics ou privés.

1  
2  
3  
4  
5  
6  
7  
8  
9  
10  
11  
12  
13  
14  
15  
16  
17  
18  
19

# $\kappa$ -carrageenan associated with

## Fructose/Glycerol/Water LTTM: towards natural thermosensitive physical gels

*Benoit Caprin<sup>†,‡</sup>, Guadalupe Viñado-Buil<sup>†</sup>, Guillaume Sudre<sup>†</sup>, Xavier P. Morelle<sup>†</sup>, Fernande  
Da Cruz-Boisson<sup>†</sup>, Aurélia Charlot<sup>\*†</sup>, Etienne Fleury<sup>†</sup>*

<sup>†</sup> Univ Lyon, CNRS, Université Claude Bernard Lyon 1, INSA Lyon, Université Jean Monnet,  
UMR 5223, Ingénierie des Matériaux Polymères, F-69621 Villeurbanne Cedex, France

<sup>‡</sup> Gattefossé SAS, 36 chemin de Genas, 69804, Saint-Priest Cedex, France

\* Corresponding author: aurelia.charlot@insa-lyon.fr, Phone: +33 (0)4 72 43 63 38

**Abstract:**  $\kappa$ -carrageenan was combined to a natural Low Transition Temperature Mixture (LTTM) composed of fructose, glycerol, and water in a 1:1:5 molar ratio (FGW) to generate fully biobased physical gels through a simple method. The resulting gels can be easily prepared under various shapes. As for their hydrogel analogues, the rheological characterization of FGW-based samples evidenced a thermosensitive gelation, attributed to the formation of aggregated H-bonded helices composed of  $\kappa$ -carrageenan chains. FGW-based gels exhibit gel-sol transition temperature ( $T_{g/s}$ ) higher than the one of hydrogels with recoverable and reversible viscoelastic properties upon successive heating/cooling cycles. SAXS analysis revealed a more extended conformation of chains in FGW that leads to more physical cross-linking junction zones within the materials. Such peculiar spatial internal organization provides a mechanical reinforcement

20 demonstrated by compression tests. In conclusion, the use of FGW solvent allows for designing  
21  $\kappa$ -carrageenan physical gels with enhanced thermal and mechanical properties.

22 **Keywords:**  $\kappa$ -carrageenan, Low Transition Temperature Mixture, organogels, thermo-  
23 sensitivity

## 24 **Introduction**

25 In the context of sustainable development, polysaccharides remain a powerful and tantalising  
26 resource for biomass valorisation since they can be used to generate eco-friendly materials. In  
27 this context, such natural polymers have been combined with Deep Eutectic Solvents (DES),  
28 just through a simple mixture, usefully exploited to obtain fully biobased and biosafe materials  
29 with relevant and tunable properties.<sup>1</sup> The interest is to benefit from the unique attributes  
30 synergistically provided by the combination of natural polymers (reduced environmental  
31 impact, renewable origin, non-toxicity...) with DES solvents, more specifically their biosafe  
32 properties, their organized character and the large versatility they provide in terms of final  
33 macromolecular structure. The preparation of these novel solvents is simple since DES come  
34 from the mixture of two (or more) H-bonded low-cost molecules. When no eutectic can be  
35 clearly identified, such mixtures are classified as low transition temperature mixtures (LTTM).  
36 In particular, natural deep eutectic solvents (NaDES) can be conceived from biobased and  
37 biosafe precursors. For instance, guar gum, a vegetal galactomannan, was combined to various  
38 choline chloride (ChCl)-based DES and physical gels with elastic behavior and relevant ionic  
39 transport properties were formed from ChCl-Urea/guar mixtures.<sup>2</sup> Xanthan gum was also  
40 described as a potential gelator of ChCl-based DES.<sup>3</sup> The authors proved that the addition of  
41 water was required to obtain physical gels. It is also reported that xanthan gum NaDES-based  
42 gels exhibit a larger thermal operating window compared to hydrogels due to the involvement  
43 of water in the supramolecular structure of the NaDES.<sup>4</sup> Despite of the prominent interest to

44 explore LTTM in the polysaccharide field, the design of materials including carrageenans has  
45 not been reported yet. Carrageenans, linear sulfated polysaccharides, are mainly extracted from  
46 red algae (*Rhodophyceae*). Carrageenan chains consist of D-galactopyranose units alternately  
47 linked by  $\alpha$ -1,3 and  $\beta$ -1,4 glycosidic bonds. The repeating units are most often disaccharides  
48 and are generally distinguished by their degree of sulfation and by the presence or absence of a  
49 3,6-anhydro bridge on the  $\beta$ -1,4-linked galactose unit. The three mostly studied carrageenans  
50 are  $\kappa$ ,  $\iota$  and  $\lambda$ -carrageenan.  $\kappa$ -carrageenan is particularly interesting since it not only finds  
51 applications in food, cosmetic and pharmaceutical industries but it leads to hard gels in aqueous  
52 medium.<sup>5</sup> It is accepted that the gelation of  $\kappa$ -carrageenan in water is achieved by a two-step  
53 thermo-dependent mechanism. Upon cooling, a coil-to-helix transition occurs, followed by the  
54 aggregation of helices, resulting in a gelation.<sup>6</sup> This gelation has been investigated by  
55 rheological and micro differential scanning calorimetry, which allowed to determine the  
56 thermal transitions : from solution to gel ( $T_{s/g}$ ) and from gel to solution ( $T_{g/s}$ ).<sup>7</sup> The influence of  
57 the nature of the solvent on the thermal transitions was also examined by Yang *et al.* by  
58 additions of sucrose or ethanol in water solutions.<sup>8,9</sup> Their investigation emphasized that the  
59 nanostructure of gels was affected by the solvent.

60 In this context, we propose herein a new study dealing with the association of  $\kappa$ -carrageenan  
61 and a novel green solvent, namely a neutral low transition temperature mixture, composed of  
62 bio-sourced and non-toxic molecules: Fructose (F), Glycerol (G), and Water (W). Indeed, we  
63 recently reported by means of DSC, rheology, and NMR spectroscopy, that FGW in 1:1:5 molar  
64 ratio (subsequently named FGW) behaves as a cooperatively H-bonded supramolecular  
65 structure leading to a stable solvent identified as LTTM exhibiting a unique and low  $T_g$ , and an  
66 outstanding microbiological stability.<sup>10</sup> Moreover, this composition was industrially  
67 implemented to efficiently extract bioactives substances from plants for cosmetic  
68 applications.<sup>11</sup> Due to its appealing advantages in terms of structuration, polarity, and ability to

69 develop synergetic interactions between its compounds, we pursue as statement of hypothesis  
70 that FGW constitutes a well-suited solvent to generate, when mixed with  $\kappa$ -carrageenan, soft  
71 materials with improved thermo-reversible properties, and reinforced mechanical behavior,  
72 compared to water-based systems.

73 In this work, we evidence for the first time the straightforward formation of physical gels based  
74 on the incorporation of  $\kappa$ -carrageenan in FGW. In particular, we successively investigate (i)  
75 their physico-chemical properties through thermal analysis, (ii) use rheological measurements  
76 to characterize the formation of gels and to underpin the thermal dependence of the gelation  
77 mechanism, (iii) use small angle X-ray scattering experiments to elucidate their internal  
78 structure, and (iv) perform compression tests in order to validate their mechanical response. The  
79 properties of the analogous  $\kappa$ -carrageenan hydrogels were systematically analyzed and  
80 compared with our novel system, in order to gain insight into the role of FGW solvent in the  
81 structuration of the gels, which is shown to dictate the final properties. To the best of our  
82 knowledge, this is the first study dealing with soft materials resulting from  $\kappa$ -carrageenan and  
83 a fully biobased LTTM.

## 84 **Experimental**

### 85 **Materials**

86 Fructose (powder,  $M=180.16$  g/mol, purity > 99%) provided by Danisco and glycerol (liquid at  
87 25°C,  $M=92.09$  g/mol, purity > 99.5%) acquired from Oleon were used without any further  
88 purification. Deionized water (18 M $\Omega$ .cm) obtained from a Veolia Aquadem<sup>TM</sup> system was  
89 used as the third component to obtain FGW LTTM according to the recently described  
90 method.<sup>10</sup>  $\kappa$ -carrageenan was provided by Roth and was used without any further purification.  
91 Its water uptake ( $\approx 7$ wt%) and thermal decomposition temperature ( $\approx 250^\circ\text{C}$ ) were measured by

92 thermogravimetric analysis (Figure S1). Its molar mass determined by Size Exclusion  
93 Chromatography is  $M_w \approx 6.0 \times 10^5$  g/mol with a dispersity of 1.3 (Figure S2). Elementary  
94 analysis conducted by Inductively Coupled Plasma – Atomic Emission Spectrometry (ICP-  
95 AES) confirms that the counter ion of the  $\kappa$ -carrageenan used is potassium since equivalent  
96 molar quantities of sulfur and potassium were obtained (data not shown). The structure of the  
97  $\kappa$ -carrageenan was confirmed by  $^1\text{H}$  NMR analysis (Figure S3).

### 98 **Preparation of the samples**

99 The preparation is based on two main steps. The first step corresponds to the dispersion of  $\kappa$ -  
100 carrageenan into FGW at room temperature (RT), under slow mechanical stirring. RT allows  
101 to limit the water evaporation that can disturb the H-bonds of FGW. For concentration of  
102 polysaccharide higher than 15 g/L, the volume of liquid and the height of the rotor were adjusted  
103 to ensure an efficient stirring while preventing the formation of bubbles in these highly viscous  
104 solutions. The water content of  $\kappa$ -carrageenan was considered for the calculation of the total  
105 amount of polysaccharide. The resulting turbid  $\kappa$ -carrageenan/FGW mixture was stirred for 30  
106 min. The second step consists in the thermal induced gelation. The mixture was gently poured  
107 into a cylindrical recipient to prevent the formation of bubbles. The recipient was then capped  
108 and put in a temperature-controlled oven at 80°C for 3 h, in which the sample progressively  
109 became transparent. The thermal induced gelation process of  $\kappa$ -carrageenan occurred during  
110 the cooling phase down to RT. The as-formed FGW-gels were pushed out of the recipient and  
111 transparent cylindrical samples were finally obtained as illustrated in Figure 1. The same  
112 procedure was applied to generate hydrogels by replacing FGW solvent by deionized water. By  
113 convenience, the carrageenan concentration is usually discussed in mass fractions (wt%) in the  
114 literature. However, in this study the concentration is expressed in g/L as FGW is denser than  
115 water ( $d = 1.3$ ).

## 116 **Characterizations**

### 117 *Differential scanning calorimetry (DSC)*

118 DSC analyses were carried out on a DSC-Q22 device (TA Instruments). Samples were placed  
119 in aluminium hermetic pans at room temperature. Thermal analyses were performed under  
120 nitrogen flow (50mL/min) and samples were submitted to 4 temperature cycles with a ramp  
121 rate of 10°C/min: 1) from 25°C down to -140°C; 2) from -140°C up to 100°C; 3) from 100°C  
122 down to -140°C; 4) from -140°C up to 25°C. The glass transition temperature ( $T_g$ ) was  
123 determined from the second heating ramp and the midpoint of the thermal transition was  
124 considered. The melting temperature ( $T_m$ ) value of hydrogels was collected from the first  
125 heating run and the maximum of the thermal transition was considered.

### 126 *Rheology*

127 The shear viscosity ( $\eta$ ) measurements were carried out on a DHR2 controlled stress rheometer  
128 (TA Instruments) operating in flow mode and using two different geometries according to the  
129 viscosity of the mixtures: *i*) an aluminium cone/plate geometry (diameter 40 mm, angle 2°, gap  
130 52  $\mu$ m) for viscosities higher than 2 Pa.s and *ii*) an aluminium concentric cylinders geometry  
131 (bob diameter x length : 28.03 x 42.11 mm, cup diameter 30.36 mm) for viscosities lower than  
132 2 Pa.s. The temperature was precisely controlled by a high-power Peltier system. Dynamic  
133 viscoelastic properties were determined with the same rheometer using a plate/plate geometry  
134 (diameter 40 mm, gap 460  $\mu$ m). All dynamic rheological data were checked as a function of  
135 strain amplitude to ensure that the measurements were performed in the linear domain.  
136 Typically, the applied strain during the dynamical measurements was settled at 1%.  
137 Temperature sweep on gels was realized in the same conditions (F=1Hz, strain=1%). The  
138 samples were carefully loaded on the Peltier plate regulated at 20°C and covered with a home-  
139 made cover to prevent evaporation. The temperature was then increased by a controlled

140 temperature ramp to a maximum temperature depending on the analysed sample (see discussion  
141 part). Then, the temperature was decreased with the same ramp to examine the reversibility  
142 with temperature. For the highest concentrations of  $\kappa$ -carrageenan in FGW, multiples thermal  
143 cycles (heating and cooling) were performed. All rheological data were processed with Trios,  
144 TA instruments software.

#### 145 *Small angle X-ray scattering analysis (SAXS)*

146 SAXS measurements were performed at the European Synchrotron Radiation Facility (ESRF,  
147 Grenoble, France) on D2AM beamline. Samples were placed between 250  $\mu\text{m}$  Kapton foils  
148 stuck on 1.6-mm-thick washers. Measurements were performed on samples equilibrated at  
149 either 20°C or 80°C. The incident photon energy  $E$  was set to 17.000 keV ( $\Delta E/E= 10^{-4}$ ). The  
150 SAXS intensity was collected using a 2D D5 detector which was placed at a sample-to-detector  
151 distance of  $D = 1.57$  m, leading to a  $q$ -range from 0.01 to 0.2  $\text{\AA}^{-1}$ . The two-dimensional data  
152 were obtained by considering the detector geometry and its flat field response. The position of  
153 the direct beam was determined with attenuators. The  $q$ -calibration was performed thanks to a  
154 silver behenate standard. The corrected two-dimensional data were averaged azimuthally to  
155 obtain intensity vs scattering vector  $q$  ( $q = (4\pi/\lambda) \cdot \sin(\theta)$ , where  $2\theta$  is the scattering angle and  $\lambda$   
156 is the incident wavelength). Finally, the scattering data were corrected for the scattering from  
157 the empty cell (Kapton windows) and normalized by the thickness and attenuation of the  
158 samples. The contribution from the solvent (FGW or Water) was subtracted.

#### 159 *Compression tests*

160 Compression measurements were performed on a double-column Instron universal testing  
161 machine at room temperature with a 500 N load cell. The cylindrical gel samples (12 mm height,  
162 20 mm diameter) were set on the lower plate and compressed by the upper plate. The  
163 compression was conducted at a constant rate of 1 mm/min to obtain engineering stress –

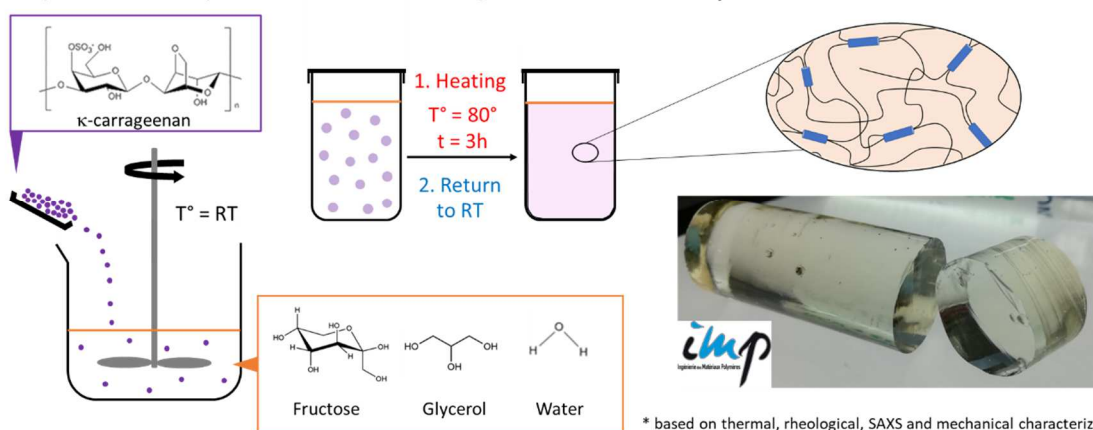
164 engineering strain curves. The compression experiments were conducted in three replicates for  
165 each gel system.

## 166 **Results and Discussion**

### 167 **Preparation of the samples**

168 Based on the literature dealing with  $\kappa$ -carrageenan hydrogels<sup>12</sup>, the gels formed with the ternary  
169 biobased FGW mixture, or deionized water as solvent were prepared according to a  
170 straightforward method described in experimental section (§2.2). At high  $\kappa$ -carrageenan  
171 concentration ( $C = 26.5 \text{ g/L} = 2 \text{ wt\%}$  in FGW and  $2.65 \text{ wt\%}$  in water), transparent soft materials  
172 with a macroscopically gel-like behavior were obtained without further processing (see picture  
173 in Figure 1). The resulting FGW-gels can be easily prepared under various shapes.  
174 Comparatively to hydrogels, FGW-gels appear less slippery, less prone to syneresis, and exhibit  
175 a better long-lasting physical stability without FGW exudation with time. This good  
176 dimensional stability can be ascribed to favorable and strong enough interactions (mainly H-  
177 bonds) between polysaccharide chains and FGW solvent (see vide-infra). Another crucial point  
178 is that FGW-based gels display an excellent microbiological stability compared to its hydrogel  
179 analogues. To conclude, an easy-to-implement and robust preparation protocol was used to  
180 obtain fully biobased gels based on polysaccharide and this natural LTTM mixture.

1. Polysaccharide dispersion → 2. Thermal gelation → 3. Physico-chemical characterization\*



\* based on thermal, rheological, SAXS and mechanical characterization

181

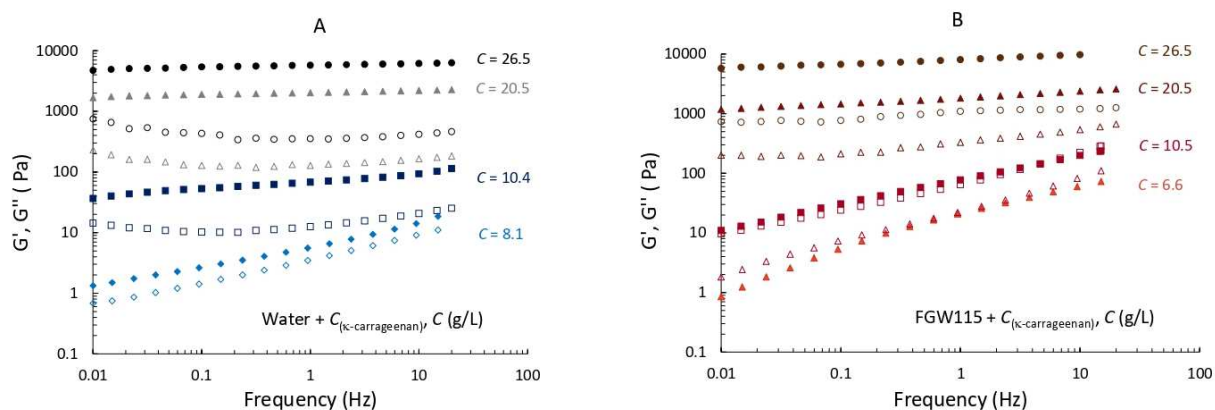
182 **Figure 1.** Illustration of the two steps procedure of  $\kappa$ -carrageenan/FGW gels: 1) dispersion of  
 183  $\kappa$ -carrageenan at room temperature, 2) heating at  $80^\circ\text{C}$  for 3h, and gelation by cooling down to  
 184 RT. The same procedure was applied to obtain hydrogels. 3) Picture of the  $\kappa$ -carrageenan/FGW  
 185 gel.

186 As recently described, the solvent FGW, classified as a natural LTTM, is characterized by a  
 187 single and low glass transition temperature ( $T_g$ ) at  $-80^\circ\text{C}$ .<sup>10</sup> DSC analyses were then applied to  
 188 evaluate the impact of  $\kappa$ -carrageenan addition on FGW thermal properties. Examples of  
 189 thermogram are given in Figure S4, for a gel prepared in FGW, in comparison with the  
 190 corresponding hydrogel. It appears that during the heating cycles, the hydrogel presents at  $7^\circ\text{C}$   
 191 a thermal event attributed to the melting of iced water when temperature varies from  $-140^\circ\text{C}$  to  
 192  $100^\circ\text{C}$ , whereas the FGW-gel only exhibits a  $T_g$  at  $-79^\circ\text{C}$ , related to the  $T_g$  of FGW. The  
 193 presence of such unique  $T_g$  value reflects the monophasic character of the mixture and shows  
 194 that polysaccharide chains do not deeply disturb the intrinsic organization of FGW solvent. We  
 195 can note that no other thermal transition can be clearly identified in these DSC thermograms.  
 196 Interestingly, the DSC analysis shows that the FGW-based samples are not subjected to any  
 197 phase transition related to water, which extends their operating temperature range.

198

199 **Rheological characterization**

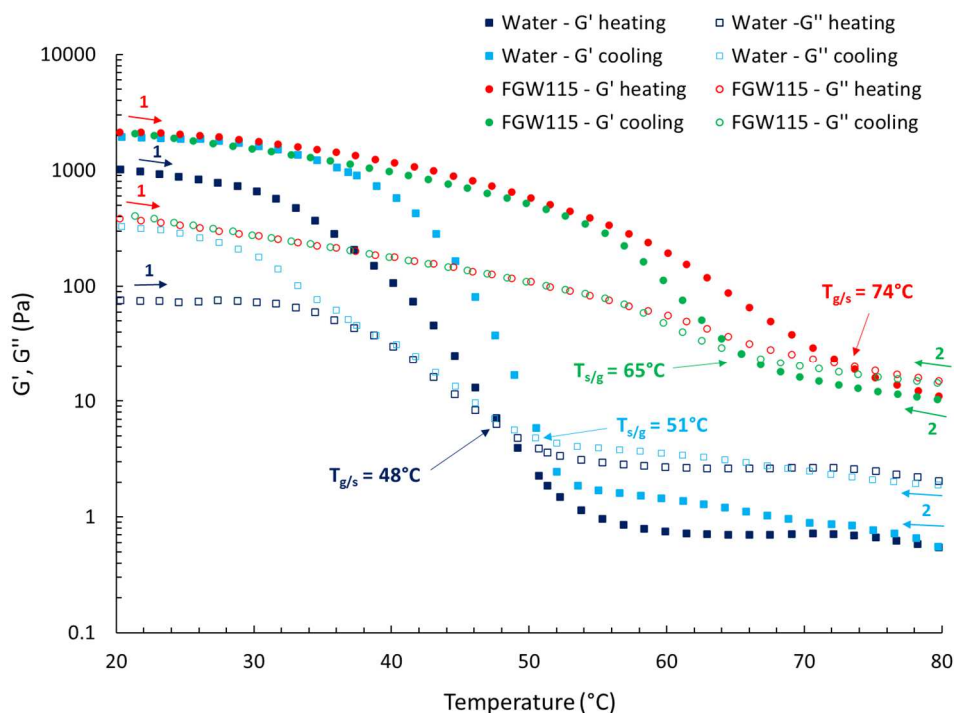
200 Rheological properties of  $\kappa$ -carrageenan-based systems were investigated. Firstly, the evolution  
 201 of viscosity with shear rate, in water and in FGW, was examined at low concentrations ( $C < 12$   
 202 g/L) (Figure S5). No macroscopical gel-behavior is observed either in water or in FGW. For  $C$   
 203  $< 5$  g/L, the aqueous solutions exhibit a Newtonian plateau. A shear-thinning behavior is  
 204 observed for larger concentrations. Conversely, FGW-based mixtures display a shear-thinning  
 205 behavior even at low concentrations (0.6 g/L). At this concentration, the viscosity of FGW  
 206 sample is two decades higher than the water-based one. This can be attributed first to the  
 207 intrinsically higher viscosity of FGW, but also to the formation of peculiar interactions between  
 208 the  $\kappa$ -carrageenan chains and/or a different chain conformation in FGW. To gain more insights  
 209 into the rheological behavior of samples based on higher chains concentrations, the frequency  
 210 dependence of  $G'$  and  $G''$  was examined in water and in FGW at 20°C for various ranges of  
 211 concentrations ( $C$  from 8.1 to 26.5 g/L in water, and from 6.6 to 26.5 g/L in FGW) (Figure 2 A  
 212 and B, respectively).



213  
 214 **Figure 2.** Frequency-dependence of  $G'$  (filled symbols) and  $G''$  (open symbols) at different  
 215 concentrations ( $C$  in g/L) of  $\kappa$ -carrageenan in water in blue (A) and in FGW in red (B) at 20°C  
 216

217

218 Regarding the aqueous samples, at  $C = 8.1$  g/L,  $G'$  is higher than  $G''$  within the entire detected  
219 frequency range, but the moduli remain sensitive to the frequency, by following a relatively  
220 close frequency dependence ( $G'$  and  $G'' \propto f^{0.4}$ ) which is typical of a transition towards a solid-  
221 like behavior.<sup>13</sup> For higher concentrations, the samples behave as physical gels as  $G'$  is  
222 significantly larger (about one order of magnitude) than  $G''$  with no strong variation of both  
223 moduli with frequency.  $G'$  reaches  $\sim 5000$  Pa at  $C = 26.5$  g/L (Figure 2A), which is consistent  
224 with values reported in the literature (2000 and 7000 Pa for 20 and 30 g/L, respectively).<sup>7</sup> For  
225 FGW-based samples, the viscoelastic response is different. The gel point ( $G' \propto G'' \propto f^{0.4}$ ) was  
226 observed to occur at higher concentration ( $C = 10.5$  g/L). Above this concentration, physical  
227 gels, characterized by a high  $G'/G''$  ratio are obtained and the previous “weak gels”, as  
228 classified by Clark & Ross-Murphy, shift to more cohesive gels when the polysaccharide  
229 concentration increases.<sup>14</sup> It is well accepted in the literature that the gelation of  $\kappa$ -carrageenan  
230 in water results from the formation of double-stranded helices laterally arranged in aggregates.<sup>6</sup>  
231 From this comparison of the viscoelastic properties, it appears that the critical  $\kappa$ -carrageenan  
232 concentration required for the aggregation of helices to occur is higher in FGW than in water.  
233 For concentrations above 20 g/L, the storage moduli in both solvents are quite similar with a  
234  $G'$  value slightly higher in FGW, compared to water (Figure 2B). These striking similarities  
235 regarding the overall viscoelastic response suggest similar gelation mechanism in the two  
236 solvents. It is well known that the rheological properties of  $\kappa$ -carrageenan hydrogels are  
237 thermally sensitive.<sup>7,15</sup> Consequently, the evolution of  $G'$  and  $G''$  as a function of temperature  
238 upon successive heating-cooling sweep was evaluated. Additionally, the influence of the  
239 polysaccharide concentration on these transition regions was also examined. From the  
240 rheological data at 20°C, a concentration in  $\kappa$ -carrageenan of 20.5 g/L was selected to study the  
241 temperature dependence of  $G'$  and  $G''$  (Figure 3).



243

**Figure 3.** Evolution of the storage  $G'$  (filled symbols) and loss  $G''$  (open symbols) moduli as a function of temperature during a heating (1) and cooling (2) rate ( $2^{\circ}\text{C}/\text{min}$ ),  $C = 20.5 \text{ g/L}$  of  $\kappa$ -carrageenan in FGW (red and green symbols) and in water (blue and light blue symbols). The thermal transitions directly indicated in the figure correspond to the crossover point of  $G'$  and  $G''$ .

244 Focusing on the hydrogel case, upon heating from  $20^{\circ}\text{C}$  up to  $80^{\circ}\text{C}$  (dark blue squares, Figure  
 245 3),  $G'$  is higher than  $G''$  at  $20^{\circ}\text{C}$  (as previously shown, see Figure 2A) but in the temperature  
 246 range between  $35^{\circ}\text{C}$  and  $55^{\circ}\text{C}$ ,  $G'$  and  $G''$  sharply decrease of around 3 decades and 1.5  
 247 decade, respectively.  $G''$  becomes greater than  $G'$  for  $T > 48^{\circ}\text{C}$ , indicating a liquid-like  
 248 behavior. This substantial decrease of both moduli has been ascribed to the thermal-induced  
 249 dissociation of the helices-based aggregates<sup>16</sup> through the progressive disruption of hydrogen  
 250 bonds by temperature increase, causing the breakage of the network. The temperature  
 251 corresponding to the  $G'$ ,  $G''$  crossover point, indicator of the gel-solution transition temperature  
 252 ( $T_{g/s}$ ), was determined to be  $48^{\circ}\text{C}$  which is consistent with the literature.<sup>7</sup> The viscoelastic

253 response of the hydrogel was then monitored upon an immediate cooling after the first heating  
254 ramp. Back at low temperatures, pronounced differences in the  $G'$  and  $G''$  values between the  
255 heating and cooling ramp emerge, which come from water evaporation during the analysis.  
256 Literature reported thermal hysteresis phenomenon ascribed to a different kinetic organization  
257 of the polysaccharide helices during heating and cooling, resulting in two different thermal  
258 transition temperatures.<sup>17</sup> Figure 3 emphasizes a quite small thermal hysteresis of 3 °C, as a  
259 value of  $T_{s/g}$  of 51 °C was recorded (light blue squares). This hysteresis is lower than the one  
260 described in bibliography, which can reasonably be explained by an overestimation of  $T_{s/g}$  value  
261 due to water evaporation. The FGW-gel, at similar concentration, was analyzed following the  
262 same thermal procedure. As shown by Figure 3, differences in the thermal behavior are  
263 observed. Firstly, the decrease of  $G'$  and  $G''$  of the FGW-gel upon the heating ramp is less  
264 acute (two decades against three decades in water for  $G'$ ). Secondly, the decrease of the moduli  
265 spreads over a larger range of temperature, with a smooth decrease from 35 °C to 52 °C  
266 followed by a more pronounced one from 52 °C up to 80 °C. Thirdly, the FGW-gel exhibits a  
267 better solvent retention propensity: after the two temperature cycles,  $G'$  and  $G''$  are perfectly  
268 superimposed, and the initial viscoelastic properties are fully recovered (Figure 3 red and green  
269 data points at low temperature). The  $T_{g/s}$  of 74 °C of the FGW-gel, determined upon the heating  
270 sweep is noticeably higher than in water, and a significant hysteresis (9 °C) appears with a  $T_{s/g}$   
271 identified at 65 °C. The  $T_{s/g}$  values of  $\kappa$ -carrageenan hydrogels are known to decrease while  
272 increasing the temperature rate and increase with increasing concentration.<sup>7</sup> Thus, we analyzed  
273 two FGW-gels ( $C = 20.5$  and  $26.5$  g/L), at various temperature ramps (1, 2 and 10 °C/min)  
274 (Table 1). The global expected trend is observed, but some small discrepancies appear for these  
275 values measured from the crossover of  $G'$  and  $G''$ . To complete these data, we also conducted  
276 another approach to determine the gelation temperature, based on the divergence of the complex  
277 viscosity ( $\eta^*$ ) during the cooling ramp, method described in detail by Liu *et al.* for hydrogels

278 (Figure S6). The resulting  $T_{s/g}$  values are quite lower than the ones collected from the crossover  
 279 method, probably due to the pronounced dispersive character of the thermal transitions within  
 280 the FGW gels. Interestingly, this series of data better fits with the expected effect of  
 281 concentration and temperature rate.

κ-carrageenan concentration	Temperature rate (°C/min)	Determination of $T_{s/g}$ (°C)	
		Method 1 G' & G'' crossover	Method 2 $\eta^*$
20.5 g/L ( $\approx$ 1.6 wt%)	1	88	69
	2	65	68
	10	78	64
26.5 g/L ( $\approx$ 2.0 wt%)	1	87	76
	2	70	73
	10	81	71

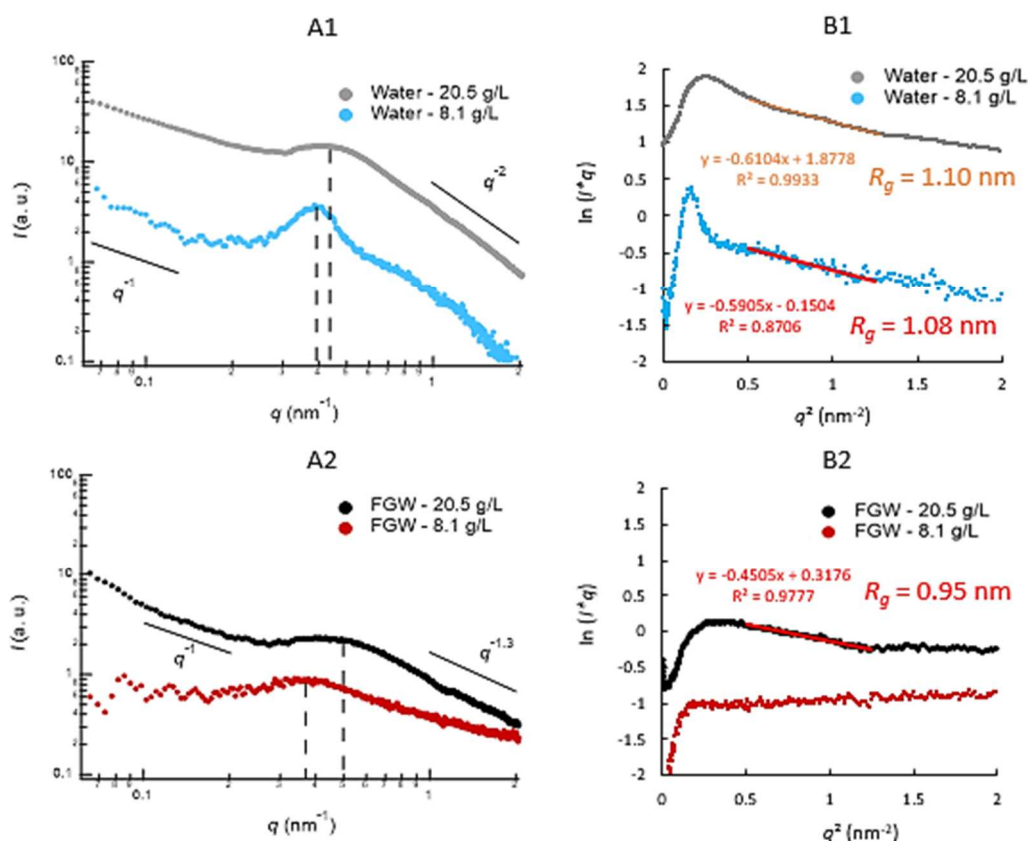
282  
 283 **Table 1.** Comparison between two methods for the determination of  $T_{s/g}$  value for two  
 284 concentrations of κ-carrageenan in FGW ( $C = 20.5$  and  $26.5$  g/L) at three different temperature  
 285 ramps (1, 2 and  $10$  °C/min). All experiments were performed at a fixed frequency of 1 Hz with  
 286 a constant strain of 1%.

287 Finally, irrespective of the employed method,  $T_{s/g}$  of FGW-gels are higher than the ones  
 288 measured for the hydrogels. Thus, a higher temperature is required in FGW to allow both the  
 289 dissociation of helices aggregates and the helix-to-coil transition. Indeed, the high viscosity of  
 290 FGW solvent, compared to water, requires a more substantial temperature input to impart a  
 291 sufficient motion of polysaccharide chains. Additionally, a FGW-gel ( $C = 26.5$  g/L) was  
 292 subjected to several heating/cooling cycles at  $10$  °C/min between  $40$  and  $100$  °C. These cycles  
 293 were applied either successively (Figure S7A), or after different waiting times between each  
 294 cycle (Figure S7B). Figure S7 highlights a complete reversibility of the viscoelastic properties,  
 295 which underpins that the kinetics of the thermal-induced disorganization / reorganization of the  
 296 cross-linked zones is rapid and confirms the high solvent retention with temperature for FGW  
 297 gels, compared to hydrogels.

298

## 299 Nanostructure of the materials

300 SAXS measurements were performed to obtain further structural information on the different  
301 gels. FGW-gels and hydrogels, at two different chain concentrations ( $C = 8.1$  and  $20.5$  g/L)  
302 were analyzed at  $20^\circ\text{C}$  (Figure 4). These concentrations were selected so that the resulting  
303 mixtures exhibit different viscoelastic behaviors. Below a polysaccharide concentration of  $10$   
304 g/L, viscoelastic liquids were obtained in FGW while "weak" gels started to be formed in water.  
305 Conversely, for  $C > 20$  g/L and at  $20^\circ\text{C}$  ( $T < T_{g/s}$ ), physically crosslinked gels characterized by  
306  $G'$  much higher than  $G''$  are generated (see Figure 3). Figure 4A shows the corresponding SAXS  
307 patterns ( $I(q)$  vs  $q$ ) of these samples.



308

309

310

311 **Figure 4.** A. SAXS patterns at 20 °C of  $\kappa$ -carrageenan at 8.1 and 20.5 g/L in water (A1) and in  
312 FGW (A2). B. Cross-sectional Guinier plots of the SAXS patterns in water (B1) and in FGW  
313 (B2) and graphical exploitation to determine the average cross-sectional radius ( $R_g$ ) of rods  
314 composed of aggregates of  $\kappa$ -carrageenan helices.

315 All four SAXS profiles presented in Figure 4A can be divided in three parts as a function of the  
316 wavevector. For  $q < 0.3 \text{ nm}^{-1}$ ,  $I(q)$  scales with  $q^{-1}$  in water (Figure 4A1). This decrease of the  
317 scattering intensity is indicative of the presence of rod-like monodispersed structures<sup>18</sup>, which  
318 corroborates the well-accepted gelation mechanism of  $\kappa$ -carrageenan in water that results from  
319 the formation of laterally arranged double-stranded helices. Thus, the physical 3D network can  
320 be described as made of bound cylinders crosslinks.<sup>6</sup> In FGW at 8.1 g/L of  $\kappa$ -carrageenan, the  
321 intensity is somewhat constant in this  $q$ -region, which seems consistent with the fact that this  
322 sample is still a viscous liquid composed of only dissolved polysaccharide chains (*i.e.* no bound  
323 cylinder crosslinks present yet). In contrast, at 20.5 g/L in FGW, the intensity decreases with a  
324 variation of  $q^{-1}$  in a shorter region ( $0.1 \text{ nm}^{-1} < q < 0.3 \text{ nm}^{-1}$ ) and the slope is steeper at lower  $q$ -  
325 values; this result suggests that cylinders are still implied in the structure of the gel, but another  
326 structure at larger length scales is also expected.

327 Then, when  $q$  is comprised between 0.3 and  $0.7 \text{ nm}^{-1}$ , scattering patterns are characterized by a  
328 broad peak. In the case when water is the solvent, it corresponds to the polyelectrolyte peak  
329 of  $\kappa$ -carrageenan.<sup>6</sup> The peak position  $q_{\text{max}}$  is related to the correlation length between chains.  
330 As expected, the position of the polyelectrolyte peak is directly linked to the concentration of  
331  $\kappa$ -carrageenan. It is also observed that the polyelectrolyte peak becomes wider when the  
332 concentration increases. Nonetheless, by adding progressive amounts of sucrose in 2 wt%  $\kappa$ -  
333 carrageenan hydrogels, Yang *et al* reported that the polyelectrolyte peak vanished for 30 wt%

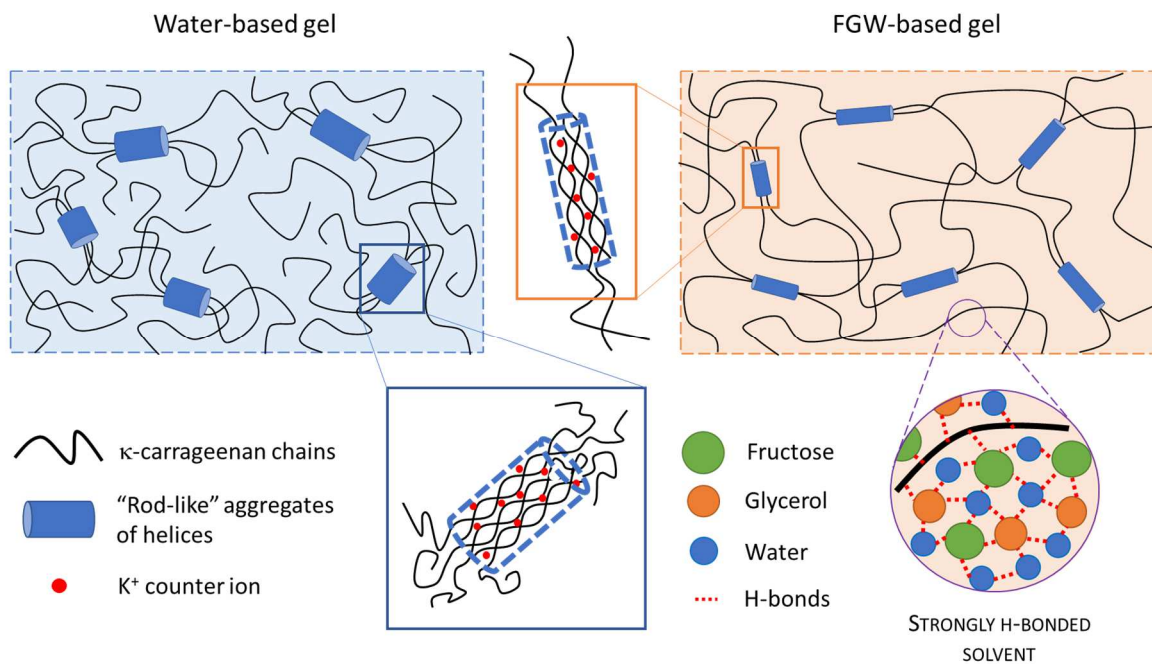
334 of sucrose. The authors argued that H-bonds between the polysaccharide and the sucrose  
335 overcame the electrostatic repulsion interactions between  $\kappa$ -carrageenan chains.<sup>9</sup> In the present  
336 study, the continuous phase (FGW) is composed of 50 wt% of fructose and ~25 wt% of glycerol  
337 and water. Despite the important number of available OH groups of the polysaccharide for  
338 developing H-bonds, a structure peak is still observed at  $q$ -values close to those of the  
339 polyelectrolyte peak observed for water-based systems. As fructose is strongly H-bonded to  
340 glycerol and water, it is less accessible to form H-bonds with the polysaccharide, as reported  
341 by Yang *et al.* for hydrogels containing sucrose.

342 Finally, when  $q$  becomes larger than  $0.7 \text{ nm}^{-1}$ , the decrease of the signal can be assigned to the  
343 propensity of the solvent to dissolve polysaccharide free chains. In this region,  $I(q)$  scales with  
344  $q^{-2}$  for water while the exponent is higher for FGW ( $\sim q^{-1.3}$ ). This suggests that the LTTM is a  
345 better solvent than water for the  $\kappa$ -carrageenan chains.

346 To gain more insight into the dimensions of junction zones at the origin of the formation of the  
347 physically cross-linked gels, cross-sectional Guinier plots ( $\ln(q.I(q))$  vs  $q^2$ ) were performed.  
348 Such representation has often been used in studies reporting the nanostructure of carrageenan  
349 hydrogels. Scattering from a long rod with a cross-sectional radius of gyration  $R_g$  is given by  
350 the Guinier approximation as  $q.I(q) \approx \exp(-q^2.R_g^2/2)$ .<sup>19</sup>  $R_g$  can thus be evaluated from the linear  
351 region in cross-sectional Guinier plots ( $qR_g < 1$ ). Figure 4B shows the cross-sectional Guinier  
352 plots obtained in water and in FGW for the two different studied  $\kappa$ -carrageenan concentrations  
353 (8.1 and 20.5 g/L). On the one hand, in the case of water, a linear region appears after the peak  
354 due to the electrostatic interactions at lower  $q$  values. The cross-sectional radius of gyration  
355 obtained are equivalent for the two concentrations (1.08 nm and 1.1 nm) (Figure 4B1), which  
356 is line with the values reported by Yang *et al.* This result indicates that the number of rods  
357 distributed in the aqueous phase increases, but the average diameter of the helices aggregates

358 remains constant. On the other hand, Figure 4B2 shows the cross-sectional Guinier plots  
359 obtained in FGW. As discussed before, only rare aggregates may be present in the solution of  
360 lowest concentration. Thus, no  $R_g$  value can be determined in this case. Conversely, the Guinier  
361 plot for the FGW gel at  $C = 20.5$  g/L yields a cross-sectional radius of 0.95 nm. SAXS profiles  
362 were also investigated at 80°C for all samples, the Guinier plots obtained at this temperature  
363 for  $C = 20.5$  g/L (data not shown) present the same profile that for the lower concentration in  
364 FGW (Figure 4B2) suggesting the disappearance of aggregates induced by the temperature  
365 increase. This is consistent with rheological measurements and the thermo-reversible behavior  
366 of  $\kappa$ -carrageenan gels (Figure 3). Eventually, it appears once again that the gelation mechanism  
367 resulting from the formation of laterally arranged double-stranded helices is quite similar  
368 between FGW and water solvents, leading to rod-like structure with similar size. Since the  
369 structure peak of the polysaccharide is broader in FGW, the distribution of interaction lengths  
370 is less dispersed in space in the case of water. We thus propose, in Figure 5, the following  
371 schematic representation of the internal organization of the hydrogel and FGW gels, mainly  
372 based on SAXS investigation but corroborated by the observed rheological behavior. In both  
373 gels, gelation is obtained, at low temperature and for sufficient polysaccharide concentration,  
374 when  $\kappa$ -carrageenan chains start forming rod-like aggregates acting like physical crosslinks.  
375 These physically bounded cylinders (schematized in blue in Figure 5) are made of an aggregate  
376 of double-stranded helices.<sup>6</sup> In the case of water-based gels, these aggregates are slightly larger  
377 in diameter than for FGW-based gels, with probably one extra double-stranded helix. Another  
378 difference between the two systems raises from the interactions between the solvent and the  
379 free  $\kappa$ -carrageenan chains, while in the case of hydrogels the chains are more coiled up; in the  
380 case of FGW, being a better solvent for  $\kappa$ -carrageenan chains that leads to a more extended  
381 network with more H-bonds between the solvent and chains, despite an apparently less  
382 homogeneous distribution of interactions lengths. With this overall structural picture, and

383 considering a same concentration  $\kappa$ -carrageenan chains, the FGW-based gel should lead to a  
 384 better-connected network with more physical junctions (as the physical aggregates in the  
 385 hydrogel case involved more  $\kappa$ -carrageenan helices) and stronger solvent-chain interactions  
 386 (*i.e.* strongly H-bonded solvent).



387

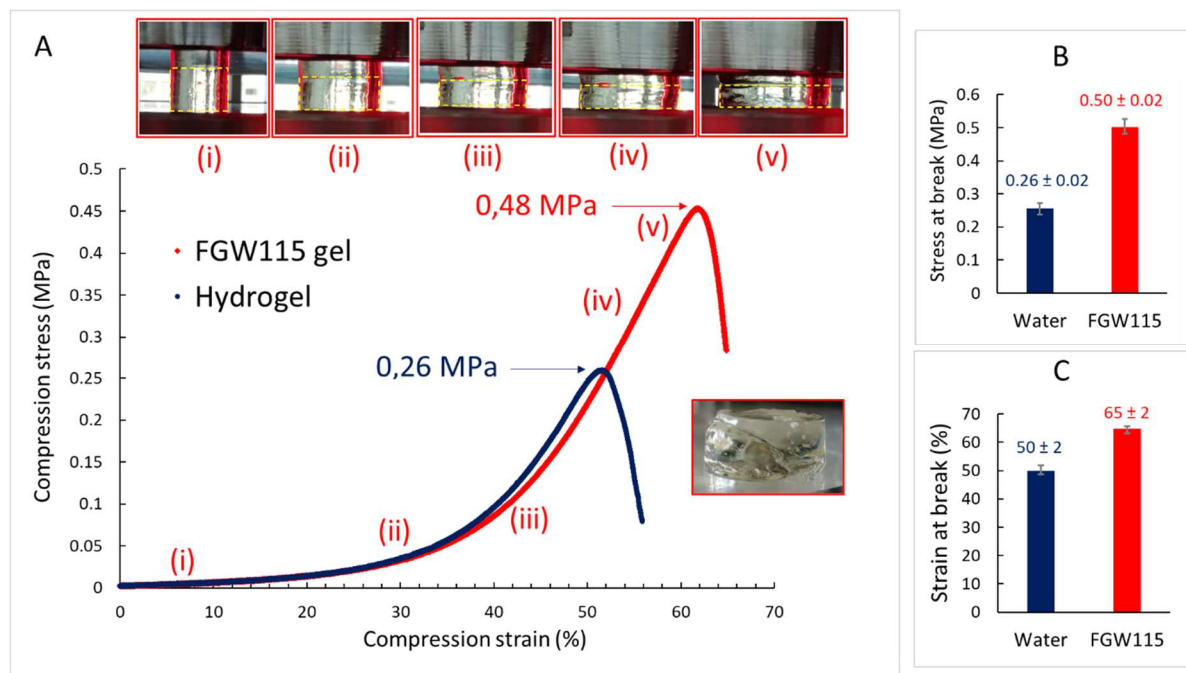
388 **Figure 5.** Illustration of the suggested organizations obtained in water-based gel and in FGW-  
 389 based gel.

### 390 Mechanical properties

391 It was reported that  $\kappa$ -carrageenan forms rigid and brittle hydrogels. When the water phase is  
 392 modified or another solvent than water is used to obtain  $\kappa$ -carrageenan gels, small deformation  
 393 tests are used to discuss the viscoelastic behavior of such mixtures. However, the mechanical  
 394 response to large deformation is scarcely described. Herein, we submitted gels obtained in FGW  
 395 and in water (26.5 g/L) to compression tests in order to reach the large strain response (see 2.3.4  
 396 Compression tests).

397 Figure 6 regroups the engineering stress – engineering strain curves obtained. As shown in this  
398 Figure, samples are progressively deformed until a maximum stress is reached, corresponding  
399 to the stress at which the gel ruptures. When samples are subjected to small strain (< 20 %), the  
400 mechanical response of hydrogel and FGW-gel are similar. This is consistent with the  
401 rheological measurements performed at small strains (see Figure 2,  $C = 26.5$  g/L): the storage  
402 modulus values obtained in both solvents are comparable. Then, for larger strains, the non-  
403 linear elastic regime of gels appears. The slope values for both solvents are relatively equivalent  
404 indicating a similar strain-hardening capacity, underlining a relatively analogous physically  
405 crosslinked gel structure. However, the range of stress supported by the FGW-gel is  
406 significantly higher than that of the hydrogel. In other words, the stress at fracture obtained in  
407 FGW (0.50 MPa) is almost twice bigger than that of the hydrogel (0.26 MPa) (Figure 6B).  
408 Concomitantly, a higher strain at break is also reported for the FGW-gel compared to the  
409 hydrogel, respectively around 65% and 50%, based on triplicate measurements (Figure 6C).  
410 For the hydrogel, the values of stress/strain at break are consistent with a previous study that  
411 reported a fracture stress of around 0.2 MPa for a 2%  $\kappa$ -carrageenan hydrogel.<sup>20</sup> In the case of  
412 FGW, despite the high compression ratio, the gel hardly exudes (compared to water),  
413 highlighting again the good solvent retention ability of the system. As the assumption of  
414 constant volume being almost respected the true stress-true strain curves are given in Figure  
415 S8. Figure S8 shows that the true strain of the FGW-gel presents a slight inflexion at large  
416 strains indicating a propensity to shear localization before rupture.

417 Thus, with a very simple preparation method, the FGW mixture proposed in this study appears  
418 as an interesting alternative to develop fully biobased gels with enhanced mechanical properties  
419 compared to hydrogels. Better properties may arise in the future for FGW-gels as Cairns *et al.*  
420 also studied the addition of carob gum to obtain tougher  $\kappa$ -carrageenan hydrogels which were  
421 better able to withstand mechanical stress.



423

424 **Figure 6.** (A) Engineering stress – strain curves obtained through compression tests at room  
 425 temperature with a compression rate of 1 mm/min for 26.5 g/L gels in water (blue line) and in  
 426 FGW (red line). (i) to (v) Pictures of the FGW-gel during compression test are shown to  
 427 illustrate its ability to reach large compressive deformation. (B) Average stress at break and (C)  
 428 average strain at break for both solvents-based gels (measurements were performed in  
 429 triplicate).

## 430 Conclusion

431 In conclusion, we were able to develop fully biosourced physical gels through the incorporation  
 432 of  $\kappa$ -carrageenan chains in FGW solvent, *via* an eco-friendly experimental approach. As  
 433 hypothesized in the introduction, FGW-based gels present improved properties compared to  
 434 their aqueous analogous. Indeed, the gels exhibit promising thermal behavior with an extended  
 435 operating temperature range compared to hydrogels. Even if the study of the nanostructure and  
 436 the rheological characterizations evidenced a similar gelation mechanism of  $\kappa$ -carrageenan in

437 both solvents, the transition temperatures  $T_{g/s}$  of the FGW-gels are higher than the ones obtained  
438 in water, and the initial viscoelastic properties are fully recovered after multiple heating and  
439 cooling cycles which is a key advantage compared to hydrogels. The supramolecular FGW  
440 structuration offers a better solvent retention and contributes to the formation of additional H-  
441 bonds within the gel. This peculiar spatial structuration provides a mechanical response  
442 improvement demonstrated by compression tests. Finally, we validate through this study, that  
443 the enhanced properties of these FGW-based gels result from the formation of synergetic  
444 interactions between this peculiar LTTM solvent and  $\kappa$ -carrageenan polymer chains. These soft  
445 materials, never reported in literature so far, are expected to find applicative uses in green and  
446 sustainable soft material technologies.

#### 447 **Conflicts of interest**

448 There are no conflicts to declare.

#### 449 **Supporting Information**

450 The supporting information part, available online, contains additional polysaccharide  
451 characterizations (TGA, SEC and NMR), and complementary physico-chemical analysis of the  
452 gels: thermal properties (DSC), rheological and mechanical properties.

#### 453 **Acknowledgements**

454 This project has received funding from Gattefossé. The authors are also thankful to Agnès  
455 Crepet (IMP, Université Claude Bernard Lyon 1) for her valuable help to obtain and process  
456 Size Exclusion Chromatography and to all technical support received at IMP lab to achieve this  
457 work. The authors also acknowledge the D2AM beamline staff at ESRF and are in debt of  
458 Isabelle Morfin (LIPhy, Grenoble) for the setup of the beamline and the initial data treatment.

459

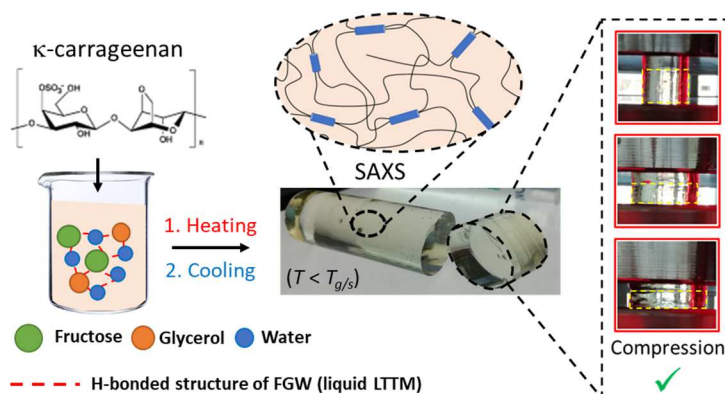
## 460 References

- 461 (1) Tomé, L. C.; Mecerreyes, D. Emerging Ionic Soft Materials Based on Deep Eutectic Solvents. *The*  
462 *journal of physical chemistry. B* **2020**. DOI: 10.1021/acs.jpcc.0c04769.
- 463 (2) Depoorter, J.; Mourlevat, A.; Sudre, G.; Morfin, I.; Prasad, K.; Serghei, A.; Bernard, J.; Fleury, E.;  
464 Charlot, A. Fully Biosourced Materials from Combination of Choline Chloride-Based Deep Eutectic  
465 Solvents and Guar Gum. *ACS Sustainable Chem. Eng.* **2019**, 7 (19), 16747–16756. DOI:  
466 10.1021/acssuschemeng.9b04228.
- 467 (3) Zeng, C.; Zhao, H.; Wan, Z.; Xiao, Q.; Xia, H.; Guo, S. Highly biodegradable, thermostable  
468 eutectogels prepared by gelation of natural deep eutectic solvents using xanthan gum:Preparation  
469 and characterization. *RSC Adv.* **2020**, 10 (47), 28376–28382. DOI: 10.1039/D0RA03390A.
- 470 (4) Xia, H.; Ren, M.; Zou, Y.; Qin, S.; Zeng, C. Novel Biocompatible Polysaccharide-Based Eutectogels  
471 with Tunable Rheological, Thermal, and Mechanical Properties: The Role of Water. *Molecules (Basel,*  
472 *Switzerland)* **2020**, 25 (15). DOI: 10.3390/molecules25153314. Published Online: Jul. 22, 2020.
- 473 (5) Zia, K. M.; Tabasum, S.; Nasif, M.; Sultan, N.; Aslam, N.; Noreen, A.; Zuber, M. A review on  
474 synthesis, properties and applications of natural polymer based carrageenan blends and composites.  
475 *International Journal of Biological Macromolecules* **2017**, 96, 282–301. DOI:  
476 10.1016/j.ijbiomac.2016.11.095. Published Online: Nov. 30, 2016.
- 477 (6) Yuguchi, Y.; Thu Thuy, T. T.; Urakawa, H.; Kajiwara, K. Structural characteristics of carrageenan  
478 gels: temperature and concentration dependence. *Food Hydrocolloids* **2002**, 16 (6), 515–522. DOI:  
479 10.1016/S0268-005X(01)00131-X.
- 480 (7) Liu, S.; Huang, S.; Li, L. Thermoreversible gelation and viscoelasticity of  $\kappa$ -carrageenan hydrogels.  
481 *Journal of Rheology* **2016**, 60 (2), 203–214. DOI: 10.1122/1.4938525.
- 482 (8) Yang, Z.; Yang, H.; Yang, H. Characterisation of rheology and microstructures of  $\kappa$ -carrageenan in  
483 ethanol-water mixtures. *Food research international (Ottawa, Ont.)* **2018**, 107, 738–746. DOI:  
484 10.1016/j.foodres.2018.03.016. Published Online: Mar. 7, 2018.
- 485 (9) Yang, Z.; Yang, H.; Yang, H. Effects of sucrose addition on the rheology and microstructure of  $\kappa$ -  
486 carrageenan gel. *Food Hydrocolloids* **2018**, 75, 164–173. DOI: 10.1016/j.foodhyd.2017.08.032.
- 487 (10) Caprin, B.; Charton, V.; Rodier, J.-D.; Vogelgesang, B.; Charlot, A.; Da Cruz-Boisson, F.; Fleury, E.  
488 Scrutiny of the supramolecular structure of bio-sourced fructose/glycerol/water ternary  
489 mixtures:Towards green low transition temperature mixtures. *Journal of Molecular Liquids* **2021**,  
490 337, 116428. DOI: 10.1016/j.molliq.2021.116428.
- 491 (11) Caprin, B.; Charton, V.; Vogelgesang, B. Chapter Twelve - The use of NADES to support  
492 innovation in the cosmetic industry. In *Advances in Botanical Research:Eutectic Solvents and Stress in*  
493 *Plants (Volume 97)*; Academic Press, 2021; pp 309–332. DOI: 10.1016/bs.abr.2020.09.009.
- 494 (12) Mangione, M. R.; Giacomazza, D.; Bulone, D.; Martorana, V.; San Biagio, P. L. Thermoreversible  
495 gelation of  $\kappa$ -Carrageenan: relation between conformational transition and aggregation. *Biophysical*  
496 *chemistry* **2003**, 104, 95–105.
- 497 (13) Richter, S. Recent Gelation Studies on Irreversible and Reversible Systems with Dynamic Light  
498 Scattering and Rheology - A Concise Summary. *Macromol. Chem. Phys.* **2007**, 208 (14), 1495–1502.  
499 DOI: 10.1002/macp.200700285.
- 500 (14) Clark, A. H.; Ross-Murphy, S. B. Structural and mechanical properties of biopolymer gels. In  
501 *Biopolymers*; Advances in Polymer Science; Springer-Verlag, 1987; pp 57–192. DOI:  
502 10.1007/BFb0023332.
- 503 (15) Mangione, M. R.; Giacomazza, D.; Bulone, D.; Martorana, V.; Cavallaro, G.; San Biagio, P. L. K(+)  
504 and Na(+) effects on the gelation properties of kappa-Carrageenan. *Biophysical chemistry* **2005**, 113  
505 (2), 129–135. DOI: 10.1016/j.bpc.2004.08.005.

506 (16) Rochas, C.; Rinaudo, M. Mechanism of gel formation in k-carrageenan. *Biopolymers* **1984**, *23*  
 507 (4), 735–745. DOI: 10.1002/bip.360230412.  
 508 (17) Ueda, K.; Itoh, M.; Matsuzaki, Y.; Ochiai, H.; Imamura, A. Observation of the Molecular Weight  
 509 Change during the Helix–Coil Transition of  $\kappa$ -Carrageenan Measured by the SEC–LALLS Method.  
 510 *Macromolecules* **1998**, *31* (3), 675–680. DOI: 10.1021/ma970846w.  
 511 (18) Hollamby, M. J. Practical applications of small-angle neutron scattering. *Phys Chem Chem Phys*  
 512 **2013**, *15* (26), 10566–10579. DOI: 10.1039/c3cp50293g. Published Online: Apr. 4, 2013.  
 513 (19) Glatter, O. Kratky, O., Ed. *Small angle X-ray scattering*; Academic Press, London, 515 p., **1982**.  
 514 (20) Cairns, P.; Morris, V. J.; Miles, M. J.; Brownsey, G. J. Comparative studies of the mechanical  
 515 properties of mixed gels formed by kappa carrageenan and tara gum or carob gum. *Food*  
 516 *Hydrocolloids* **1986**, *1* (1), 89–93. DOI: 10.1016/S0268-005X(86)80010-8.  
 517

## 518 Graphical Abstract

519 Fully biosourced physical gels with enhanced mechanical properties were obtained through an  
 520 eco-friendly and simple experimental route



521

522

For Table of Contents Only